

# A Unified Knee and Ankle Design for Robotic Lower-Limb Prostheses

Md Rejwanul Haque and Xiangrong Shen<sup>\*</sup>, *Member, IEEE*

**Abstract**— The recent development in robotic lower-limb prostheses have helped amputees restore their joint functions and enabled them to perform diverse and energetically challenging daily locomotive activities, which are usually beyond the functionality of the passive prostheses. Although robotic knee prosthesis and ankle prosthesis have their common purpose of restoring joint functions for lower-limb amputees, they have generally been treated as distinct, standalone devices. Realizing such common objective and leveraging the similarities between the knee and ankle design, in this paper, a new unified design approach is proposed, which adopts a Common Core Components Knee-Ankle Prosthesis design. This research specifically targets the robotic knee/ankle joint design unification as a major goal, while fulfilling their biomechanical requirements, especially the torque, speed, and range of motion and form factor requirements associated with the knee/ankle joints. Based on such requirements, a unified knee/ankle joint design was developed, which features an identical transmission mechanism and system layout while still providing the desired level of flexibility (joint-specific customization) through swappable timing-belt pulleys.

## I. INTRODUCTION

Development and clinical application of robotic (powered) prostheses is arguably one of the most important advances in the history of lower-limb prosthetics. With the capability of actively powering the joint movements, a robotic prosthesis may potentially provide a significantly improved performance and user experience in comparison with the traditional passive prostheses. Interestingly, robotic knee prosthesis and ankle prosthesis have largely been treated as mutually exclusive, standalone devices/products, despite their common purpose of restoring joint functions for lower-limb amputees. The typical commercial product of knee prosthesis is the Ossur POWER KNEETM, which has been in clinical use for over ten years and is currently in its second generation [1]. In comparison, the typical product of ankle prosthesis, otto bock Empower (previously BioM Ankle [2]), has a very different form factor and actuation mechanism (ball screw-based linear actuator) [3]. Perhaps such difference can be best illustrated by the above-knee prosthesis designs that comprise both powered knee and ankle joints, e.g., Vanderbilt Leg [4], Knee-ankle prosthesis developed by UT Dallas [5] and the recently developed Open-Source Leg [6]. In the Vanderbilt Leg, the powered knee joint is powered with 30-mm Maxon EC-4pole brushless dc motor, while the powered ankle is powered with 60-mm Maxon 14 pole brushless dc motor. In the UT Dallas

Knee-ankle prosthesis, both the knee and ankle joints are powered with ILM 85x26 motor kit, Robodrive, Germany, brushless dc motor. But their dissimilarity remains in the transmission system, while the knee transmission is a single-stage stepped-planet compound planetary gear transmission, the ankle transmission is a 4-bar linkage mechanism. In the Open-Source Leg, the commonality between the knee and ankle reaches a much higher level, as both joints are powered with the same flat motor. The specific transmission designs, on the other hand, remain distinctly different.

In industry, standardization has been a major trend and contributing factor for the cost reduction and improvement of in-use reliability of a wide variety of products. Considering the small volume of the lower-limb prosthesis market, unifying the knee and ankle joint designs could be especially meaningful in making the prosthetic devices easier to fabricate, easier to maintain, and more affordable for the amputee users. The research in this paper targets explicitly the joint design unification as a main goal and investigates the dual facets that dictate the robotic knee/ankle designs: 1) biomechanical requirements, especially the torque, speed, and range of motion; 2) form factor requirements associated with the knee/ankle joints. Depending on such requirements, a unified knee/ankle joint design was developed, which features a unified transmission mechanism and system layout while still providing the desired level of flexibility (joint-specific customization) through swappable timing-belt pulleys. In the following section, the biomechanical characteristics of the knee and ankle during walking are analyzed, and the results form the basis of the subsequent powered joint design.

## II. ANKLE AND KNEE BIOMECHANICS IN WALKING

The biomechanics of normal walking is very important, which provides the foundation for the design of the robotic ankle and knee prosthesis. The human level-ground walking gait cycle starts when the heel touches the ground of one foot and finishes at the subsequent heel touch of the same foot [7]. The entire gait cycle is divided into two phases - stance phase and swing phase. The stance phase contributes around 60% of the gait cycle, and the remaining 40% of the gait cycle is in the swing phase [8]. In this section, the analysis of the kinematics and kinetics in walking has been used as an important tool for quantifying lower limb joints movements and forces.

### A. Ankle Biomechanics in Walking

The key movements of the ankle joint are dorsi and plantarflexion which occur in the sagittal plane [9]. As the basis of determining the ankle range of motion, existing biomechanical data from Winter [8] are utilized to generate ankle angle trajectories for three different walking speeds

<sup>\*</sup>Research supported by National Science Foundation Grant 1734501.

M. R. Haque and X. Shen are with the Department of Mechanical Engineering, University of Alabama, Tuscaloosa, AL, USA. (corresponding author\* phone: 205-348-6743; fax: 205-348-6959; e-mail: xshen@eng.ua.edu).

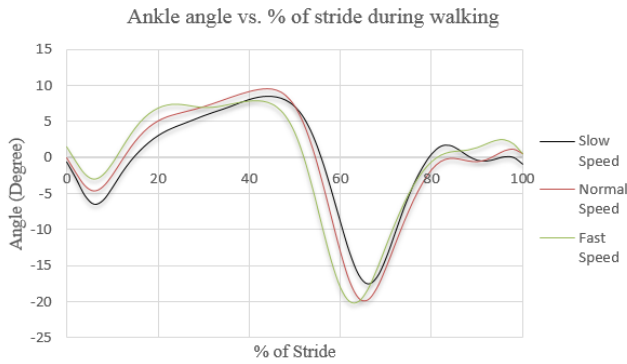


Figure 1. Ankle joint angle trajectory in level walking for slow, normal and fast speed

(slow, normal, and fast), as shown in Fig. 1. The angle trajectories indicate an overall range of motion of ankle joint between  $\sim 30^\circ$  (dorsiflexion  $\sim 9^\circ$  and plantarflexion  $\sim 20^\circ$ ). Although, the ankle range of motion varies significantly between persons due to gender, age, and ethnic differences [10], many researches have indicated a total range of motion of ankle is around  $65^\circ$ - $75^\circ$  (approximately  $40^\circ$ - $55^\circ$  and  $10^\circ$ - $20^\circ$  of plantarflexion and dorsiflexion respectively) [10], [11]. A recent study on 21 subjects (10 male and 11 female) indicates the total range of motion during walking is  $27^\circ$  ( $5^\circ$  dorsiflexion and  $22^\circ$  plantarflexion) while speed is 1.1 m/s and  $30^\circ$  ( $4^\circ$  dorsiflexion and  $26^\circ$  plantarflexion) while speed is 1.6 m/s [12]. However, in daily activities, the range of motion required is reduced to  $\sim 30^\circ$  for normal walking [8], [13].

To understand and model the way human regulates ankle torque during walking; a graphical approach of analyzing gait has been adopted. As the basis of this work, existing biomechanical data from Winter [8] are utilized to generate a trajectory on the angle-torque plane, as shown in Fig. 2. The trajectory is segmented into several of phases described below, where each phase exhibits a set of distinct dynamic characteristics.

- Controlled Plantar Flexion (A  $\rightarrow$  B): This phase begins at heel-strike (Point A), and ankle becomes flat with a small flexional torque. Such dynamic behavior can be modeled as a soft linear spring ( $\sim 0.77$  N-m/deg).
- Controlled dorsiflexion (B  $\rightarrow$  C): This phase starts at foot-flat (Point B) and ends when the ankle reaches the maximum dorsiflexion. In this process, the whole-body weight is supported on a single limb and the torque increases with the joint angle. The biomechanical joint behavior within this phase can be modeled with a very stiff virtual spring ( $\sim 7.34$  N-m/deg).
- Powered plantar flexion (C  $\rightarrow$  D): This phase starts after maximum dorsiflexion and continues until the toe-off (point D) happens. The torque starts with the maximum value and reduces to zero at the end of this phase. The biomechanical behavior of this phase can be modeled with a strong virtual spring, with the stiffness of  $\sim 4.61$  N-m/deg.

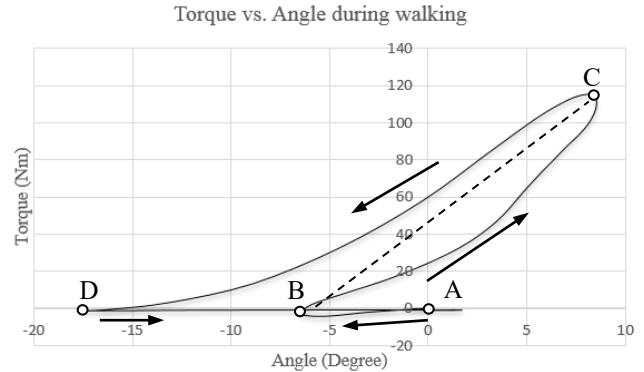


Figure 2. Ankle torque vs. angle behavior during walking for a 75Kg male subject. The condition of the foot during heel-strike, foot flat, maximum dorsiflexion and toe-off are marked as (A), (B), (C) and (D)

- Swing phase (D  $\rightarrow$  A): This phase starts with the toe-off and ankle experiences fast dorsiflexion to return to the original position of the gait cycle. The behavior of this phase can be modeled with a mild virtual spring, with the stiffness of  $\sim 0.021$  N-m/deg. Based on the biomechanical data by winter [8], the peak joint velocity is around 3 rad/s in this phase.

Based on the study in this section, the main design objective is to fulfill the actuation torque and the range of motion requirements rather than the speed requirement which is relatively slow ( $\sim 3$  rad/s) in comparison with the knee. As indicated by the biomechanical study, the peak torque (occurs at maximum dorsiflexion) is approximately 115.13 N-m, which can serve as the torque capacity for the design objective. Furthermore, the range of motion of the prosthesis should be more than  $30^\circ$  (dorsiflexion  $\sim 10^\circ$  and plantarflexion  $\sim 20^\circ$ ), to meet the joint angle range of motion requirement in walking.

### B. Knee Biomechanics in Walking

A similar graphic approach is used to model the biomechanical behavior of the knee in walking. The key movement of the knee joint complex is flexion, extension, and hyperextension occurring in the sagittal plane. Similar to ankle joint, the knee joint range of motion also varies significantly between individuals due to gender, age, and ethnic differences. As the basis of determining knee range of motion, existing biomechanical data from Winter [8] are utilized to generate a knee angle trajectory, as shown in Fig. 3. The angle trajectory indicates an overall range of motion of knee joint between  $65^\circ$ - $70^\circ$  degree. A recent study by Grimmer et al. also verifies the range of motion of knee joint between  $65^\circ$ - $70^\circ$ .

To understand and model the way humans regulates knee torque during walking, the knee angle-torque trajectory has been generated utilizing existing biomechanical data from Winter [8] as shown in Fig. 4. The trajectory is segmented into several phases described below, where each phase exhibits a set of distinct dynamic characteristics.

- Early Stance (A  $\rightarrow$  B  $\rightarrow$  A): Beginning of this phase, the knee flexed slightly ( $\sim 5^\circ$ ) with a small flexional torque ( $\sim 20$  N-m) under the initial ground contact to absorb the impact energy. During this process, the

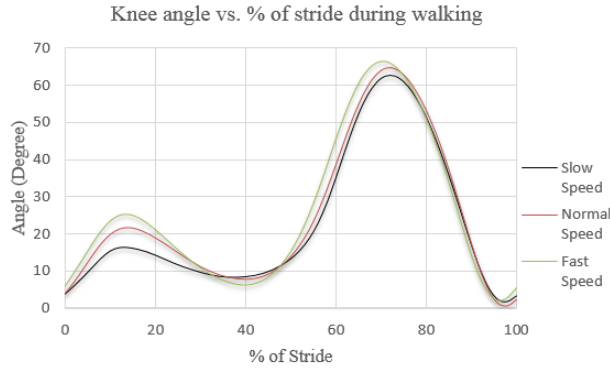


Figure 3. Knee joint angle trajectories in level walking

knee joint maintains a very high stiffness to avoid the collapse and provide steady support to the human body. After the initial ground contact at point A, the knee continues further flexion under the dynamic load until reaching the Point B (maximum flexion). In this process, the joint torque increases in and reaches the maximum extensional torque of  $\sim 45$  N-m. The biomechanical joint behavior within this phase can be modeled with a very stiff virtual spring (approximately  $5$  N-m/deg for a  $75$  kg subject).

- Pre-Swing (A  $\rightarrow$  C): In this phase, the knee experiences fast flexion ( $\sim 20^\circ$ ) to get ready for the following swing phase. In this process, the flexional torque starts at the maximum value and decreases with the joint angle until reduces to zero. The biomechanical behavior within this phase can be modeled with a soft virtual spring ( $\sim 1$  N-m/deg for a  $75$  kg subject)
- Swing flexion (C  $\rightarrow$  D). In this phase, the knee continues to flex until it reaches the maximum flexion (Point D). In this process, the joint torque decreases with the joint angle. The dynamic behavior, therefore, is mostly dissipative and thus can be modeled with a mild virtual damper. Based on the existing biomechanical data by Winter [8], the peak joint velocity is  $\sim 5$  rad/s, and the damping coefficient can be calculated as  $\sim 2.4$  N-m-s/rad.

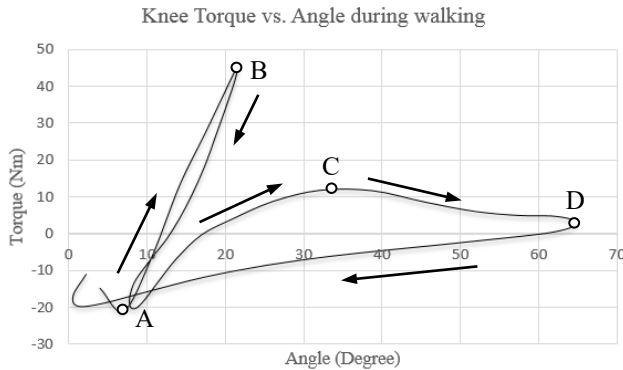


Figure 4. Knee torque vs. angle behavior during walking for a  $75$  Kg male subject. The condition of the foot during heel-strike, Maximum knee flexion during weight acceptance, Toe-off and Maximum knee flexion during the swing are marked as (A), (B), (C) and (D)

- Swing extension (D  $\rightarrow$  A). In this phase, the knee returns to the starting position (point A) by experiencing a fast extension. In this process, the knee produces a flexional torque that increases with the extension of the knee. Such behavior can be modeled with a mild virtual spring ( $\sim 0.4$  N-m/deg).

The biomechanics of the ankle and knee during walking are summarized in table I.

TABLE I. SUMMARY OF THE BIOMECHANICS DURING WALKING

Summary of the Biomechanics during walking		
	Ankle	Knee
Peak Torque (Nm)	115.13	46.125
Peak Speed (rad/sec) [12]	4.81	6.46
Range of motion (degree)	30	70

### III. BIOLOGICAL IMPLICATIONS FOR PROSTHESIS DESIGN

Ideally, the size and shape of the robotic prosthesis should be similar to the size and shape of the lost limb for aesthetic reason and most importantly for the daily use comfort. Hence, the size and shape are very crucial elements for the prosthetic device design, which are primarily determined based on the principles in human anatomy. If the length of the prosthesis is too high, then tall amputees or amputees with short residual limb can only use it. Besides, the width of the prosthesis should be compact to stay within the natural anatomical envelope. Although the volumetric profile of the limb varies significantly between persons due to gender, age, and ethnic differences, a 3D model of a 50th percentile adult male leg shown in Fig. 5, has been taken as a basis for the shape and size requirement of the prosthesis design. The knee and ankle joint width of the model are  $10.3$  cm and  $6.35$  cm respectively, whereas the joint height of the ankle is  $7.62$  cm. To keep the volumetric profile within the anatomic envelope, the target width, height, and joint height of the prosthesis have been chosen  $6.35$  cm,  $18$  cm [14] and  $7.62$  cm, respectively. Similar to the volumetric profile, the weight of the prosthesis should be within the weight of the corresponding limb segments since the heavyweight prostheses need extra metabolic energy expenditure for locomotion.

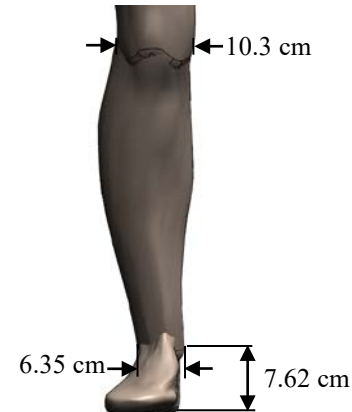


Figure 5. Human leg 3D model (Knee and Ankle front view)

To determine the weight limit of the prosthesis, a 50th percentile male subject of 75 Kg is considered. Considering the missing limb height from the ground 18cm (which is the target height of the prosthesis), the mass of the lost limb can be calculated 1.88 Kg (approximately 2.50% of the entire body mass) [8]. This mass serves as the upper limit for the mass of the prosthesis. Special attention was given to keep the weight of the prosthesis as light as possible since the standard connection to the residual limb is via vacuum socket and can become loosened by a heavier prosthesis.

#### IV. DESIGN SPECIFICATION

The biomechanics locomotion and principles of human anatomy described in the previous sections are the key tools to identify requirements for robotic prosthesis design. In this section, the target specifications for the ankle and knee design are outlined.

##### A. Ankle Design Specifications

Based on the biomechanical study, a powered ankle prosthesis is expected to meet some specific design specifications. The design specifications are based on a male subject of 75 kg weight and 1.75 m height.

- Size and mass- Based on the human anatomical analysis of the previous section, the target height and mass for the ankle prosthesis have been determined 18 cm and 1.875 Kg respectively. Additionally, the joint height and width have been determined as 7.62 cm and 6.35 cm respectively.
- Range of motion- According to the study in section II, the overall range of motion of ankle joint between has been determined as  $\sim 30^\circ$  (dorsiflexion  $\sim 10^\circ$  and plantarflexion  $\sim 20^\circ$ ).
- Torque and Speed- Based on the biomechanical study in section II, the required peak torque and speed of the ankle during walking has been determined as 115.13 N-m and 4.81 rad/s, respectively.
- Structural strength- The prosthesis must be strong enough to support the user's weight and the actuation forces from the actuators.

##### B. Knee Design Specifications

The knee design specifications are quite similar to ankle design specification except for the range of motion requirement, the torque and speed requirements. According to the biomechanical study in section II, the maximum range of motion can be as high as  $70^\circ$ . Additionally, the biomechanical study suggests that the knee needs to produce less work than the ankle, which poses less torque requirement for the knee prosthesis. On the other hand, the knee has a higher speed requirement than the ankle, which is targeted at approximately 6.46 rad/s based on the biomechanical study [12], [15].

#### V. A UNIFIED ROBOTIC PROSTHETIC JOINT DESIGN FRAMEWORK

The goal of this work is to develop a Common Core Components Knee-Ankle Prosthesis (C3KAP). The design of the C3KAP is motivated by the requirement for a compact

device that fulfills the shape, size and weight requirement of actual healthy knee and ankle, but still delivers adequately large torque and power output. This requirement poses the challenge of designing a compact actuation mechanism with a high transmission ratio. In our design (shown in Fig. 6.), two-stage transmission mechanism was chosen. The first stage was a timing belt drive transmission system, and the second stage is a harmonic drive transmission system. A commercial off-the-shelf product was chosen in the design, which is a 70 W permanent-magnet brushless motor (EC 45 flat, Maxon Motor, Sachseln, Switzerland). This motor is very light weight (141g) which can provide a peak torque of 0.20 Nm with a maximum speed of 10,000 rpm. For the second stage of transmission system, a commercial harmonic drive gear set (CSD-20-50-2A-GR, Harmonic Drive, Peabody, MA) was chosen. This harmonic drive is also lightweight and compact (13.7 mm thickness and 70 mm outer diameter) but still provides a large transmission ratio (50:1 ratio). Additionally, a cross-roller bearing (RB 2508, THK America, Schaumburg, IL) was selected to support the axial/ radial loads as well as the bending moments. All these off-the-shelf components were chosen to ensure the size and weight of the prosthesis within the target, mentioned in previous section while maintaining satisfactory performance. An easy swappable timing belt drive transmission stage was placed between the motor and the second stage. This setup helped reducing device width and provides the total gear ratio adjustability. According to the design specification mentioned earlier section, the ankle has higher torque and lower speed requirement than the knee, 4:1 time belt ratio was chosen for ankle while 3:1 ratio was chosen for the knee. By combining the two transmission stages, the total ratio becomes 150:1 for the knee and 200:1 for the ankle, generating a peak output torque of 30 Nm and 40 Nm while peak speed was 6.98 rad/s and 5.23 rad/s respectively considering negligible transmission loss. The key advantage of this transmission stage was the easy swap-ability of timing-belt pulleys, which allow a wide range of speed and torque customization for the knee and ankle. The motor of the actuation unit was attached with the input pulley of the belt drive and the output pulley was attached with the input of the harmonic drive. The output

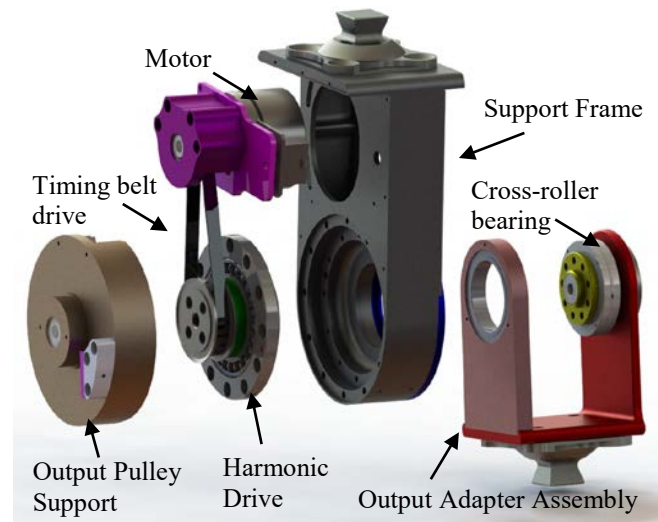


Figure 6. C3KAP actuation system (Exploded view)

pulley also included the intermediate shaft and a bearing, which was supported by Output Pulley Support. Both transmission stages were mounted on a structural part called Support Frame, which is shown in Fig. 6. The main purpose of the Support Frame is to allow mounting space for several parts and support the bending and axial loads during locomotion. The opening of the Support plate provides mounting space for the motor and input pulley assembly. The position of the motor-pulley assembly can be adjusted easily to tension the timing belt. Support Frame also features mounting arrangement for the harmonic drive, cross-roller bearing and output pulley support assembly. The circular spline of the harmonic drive is attached with an Output adapter serves as the output. The output pulley of the belt-drive stage is supported through an intermediate shaft. This output pulley is finally attached with the wave generator to

drive the harmonic drive. Additionally, the Support Frame provides a flat surface to mount the pyramid connector (standard prosthetic connector). The output adapter consists of two parts, one was an L shaped part attached directly to flexspline through the cross-roller bearing, and the other one was attached with the Output Pulley Support to share additional load of the output adapter. The output adapter provides housing for a carbon fiber footplate for ankle or standard prosthetic connector for the knee.

A special feature was added in C3KAP design, which was a unidirectional leaf spring that can generate additional push-off torque for ankle in walking. This feature is only required while the C3KAP is used as an ankle. The energetic behavior of the ankle dorsiflexion is comparable to loading a torsional spring and storing energy for push-off. This behavior can be simulated using this unidirectional leaf spring, integrated into the footplate. The leaf spring is made of carbon fiber with the stiffness of 6 Nm/deg. That means this feature greatly reduces the actuation torque requirements of the device by adding approximately 36 Nm torque during push-off.

The final design assembly of the C3KAP model for knee and ankle along with the 3D model of a 50th percentile male human leg is shown in Fig. 7.

## VI. C3KAP PROTOTYPE

The prototype of the C3KAP has been fabricated (shown in Fig. 8). To minimize the weight, high strength aluminum 7075 has been used extensively throughout the C3KAP for the structural materials. For the prosthesis control, C3KAP is instrumented with electronic components including microcontroller and sensors. To protect the internal parts, two protective 3D-printed covers were added on the prosthesis. The specifications of the developed C3KAP prototype have been summarized in Table II. By comparing these specifications with the biomechanics parameters in Table I, the range of motion, peak speed, weight, and form factor of both ankle and knee fulfill the targeted requirements. Although the torque of the ankle joint could not meet the targeted torque, it can be considered reasonable for normal ground walking.

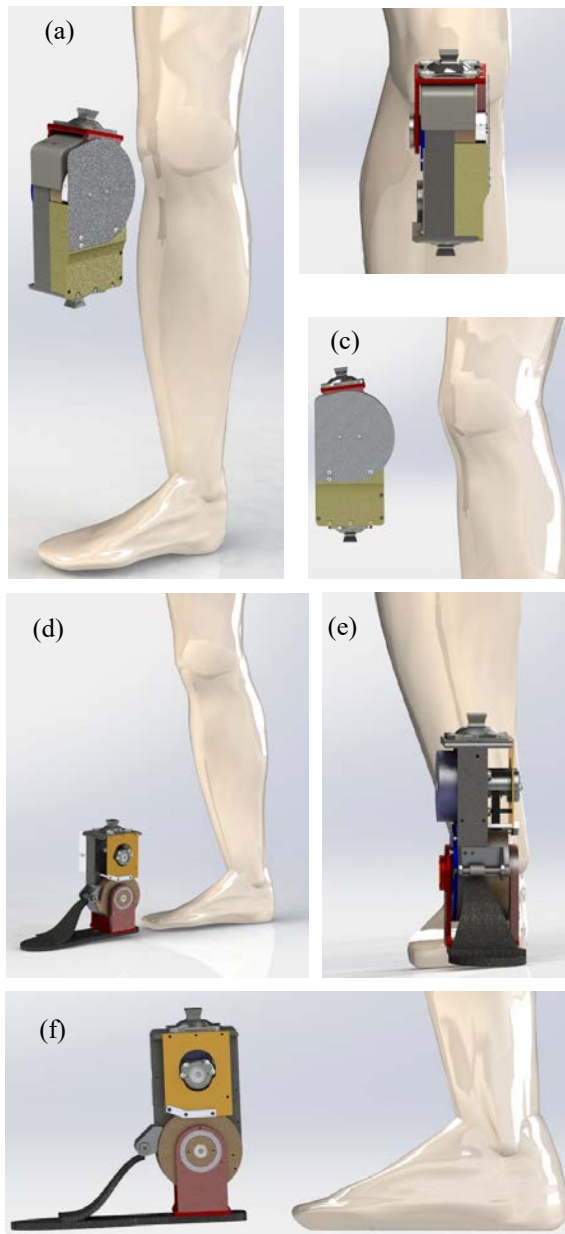


Figure 7. Human leg 3D model vs final design assembly of the C3KAP model: Knee : (a) isometric (b) front and (c) side view; Ankle : (d) isometric (e) front and (f) side view



Figure 8. C3KAP prototype (Both knee and ankle)

TABLE II. THE SPECIFICATIONS SUMMARY OF THE C3KAP PROTOTYPE

Summary of the Specification		
	Ankle	Knee
Weight (gram) (without battery)	1452	1392
Length (cm)	16.4	16.4
Width (cm)	6	6
Joint Height (cm) (from ground)	6.86	-
Peak Torque (Nm)	40 (without leaf spring)	30
	64 (with leaf spring)	
Peak Speed (rad/sec)	5.23	6.98
Range of motion (degree)	42 (dorsiflexion 12 plantarflexion 30)	-5 to 70

## VII. DISCUSSION AND CONCLUSION

This paper presents a unified knee and ankle robotic prosthesis design by introducing an identical two-stage transmission mechanism. Among the two-stage transmission, the timing-belt pulley transmission stage is easily customizable which provides a wide range of flexibility to fulfill different torque and speed requirements of the ankle and knee. In this unified design, a total of eleven components (excluding commercial off-the-components) were standardized for ankle and knee prosthesis. The proposed unified prosthesis design is able to provide majority of the actuation torque for normal walking along with the sufficient speed. Additionally, an easy installation mechanism of a unidirectional leaf spring was introduced to provide additional push-off torque of ankle during walking. Although the design was focused mostly on walking, the range of motion of the prosthesis joint satisfies the requirement for most of the ambulation modes [11], [16]. The MIT [17] and Open Source Leg [6] ankle prosthesis has a range of motion of 45° and 30° respectively which are comparable with C3KAP, while Vanderbilt ankle has even higher range of motion of 70° [4]. On the other hand, the range of motion of C3KAP knee is similar to most of the other prosthesis knee [4], [6], [17]. The speed of the knee and torque of the ankle joint may be limited for running or some other challenging tasks [9]. The speed of the C3KAP is comparable with other prosthesis while torque is lower than some prosthesis [6], [17]. Size and weight are very important factors for prosthetic device development. The volumetric profile of our developed prosthesis fits inside the anatomic envelope of the 50th percentile adult male leg. The length of our prosthesis was 16.4 cm, which will fit a wide range of amputee users. Special attention was given to keep the prosthesis width minimum as possible. The overall width of the knee and ankle prosthesis joint was 6 cm, which is within the range of average adult male and female knee and ankle joint width. On the other hand, the heavier prosthetic device requires additional metabolic energy expenditure during locomotion. The weight of our developed ankle was 1452 g and knee 1392 g (without the battery), which is lower

than most knee or ankle prosthesis [4], [6], [18], [19]. The future study includes the investigation of carbon fiber leaf spring design to provide more torque to ankle.

## REFERENCES

- [1] "POWER KNEE™." <https://www.ossur.com/en-us/prosthetics/knees/power-knee>.
- [2] "BiOM Ankle Foot System - Infinite Technologies Prosthetics," *Infinite Technologies Orthotics and Prosthetics*. <https://www.infinitetech.org/biom-ankle-foot/> (accessed May 31, 2020).
- [3] "Empower." <https://www.ottobockus.com/prosthetics/lower-limb-prosthetics/solution-overview/empower-ankle/>.
- [4] B. E. Lawson, J. Mitchell, D. Truex, A. Shultz, E. Ledoux, and M. Goldfarb, "A Robotic Leg Prosthesis: Design, Control, and Implementation," *IEEE Robot. Autom. Mag.*, vol. 21, no. 4, pp. 70–81, Dec. 2014, doi: 10.1109/MRA.2014.2360303.
- [5] T. Elery, S. Rezazadeh, C. Nesler, J. Doan, H. Zhu, and R. D. Gregg, "Design and Benchtop Validation of a Powered Knee-Ankle Prosthesis with High-Torque, Low-Impedance Actuators," in *2018 IEEE International Conference on Robotics and Automation (ICRA)*, May 2018, pp. 2788–2795, doi: 10.1109/ICRA.2018.8461259.
- [6] A. F. Azocar, L. M. Mooney, L. J. Hargrove, and E. J. Rouse, "Design and Characterization of an Open-Source Robotic Leg Prosthesis," in *2018 7th IEEE International Conference on Biomedical Robotics and Biomechanics (Biorob)*, Aug. 2018, pp. 111–118, doi: 10.1109/BIOROB.2018.8488057.
- [7] I. V. T, R. H. J, and T. F., *Human Walking*. Baltimore: Williams & Wilkins, 1981.
- [8] D. A. Winter, *Biomechanics and motor control of human gait: normal, elderly and pathological - 2nd edition*, vol. Ed2. 1991.
- [9] H. Zwiip and T. Randt, "Ankle joint biomechanics," *Foot Ankle Surg.*, vol. 1, no. 1, pp. 21–27, 1994, doi: 10.1016/S1268-7731(05)80052-9.
- [10] S. K. Grimston, B. M. Nigg, D. A. Hanley, and J. R. Engsborg, "Differences in Ankle Joint Complex Range of Motion as a Function of Age," *Foot Ankle Int.*, vol. 14, no. 4, pp. 215–222, 1993, doi: 10.1177/107110079301400407.
- [11] R. N. Stauffer, E. Y. S. Chao, and R. C. Brewster, "Force and motion analysis of the normal, diseased, and prosthetic ankle joint," *Clin. Orthop.*, vol. NO. 127, pp. 189–196, 1977.
- [12] M. Grimmer, A. A. Elshamhory, and P. Beckerle, "Human Lower Limb Joint Biomechanics in Daily Life Activities: A Literature Based Requirement Analysis for Anthropomorphic Robot Design," *Front. Robot. AI*, vol. 7, 2020, doi: 10.3389/frobt.2020.00013.
- [13] M. Nordin and V. H. Frankel, *Basic Biomechanics of the Musculoskeletal System*. Lippincott Williams & Wilkins, 2001.
- [14] R. S., *Prosthetics and Orthotics: Lower Limb and Spine*. Lippincott Williams & Wilkins, 2002.
- [15] D. A. Winter, "Biomechanical motor patterns in normal walking," *J. Mot. Behav.*, vol. 15, no. 4, pp. 302–330, Dec. 1983, doi: 10.1080/00222895.1983.10735302.
- [16] G. Bovi, M. Rabuffetti, P. Mazzoleni, and M. Ferrarin, "A multiple-task gait analysis approach: kinematic, kinetic and EMG reference data for healthy young and adult subjects," *Gait Posture*, vol. 33, no. 1, pp. 6–13, Jan. 2011, doi: 10.1016/j.gaitpost.2010.08.009.
- [17] S. K.-W. Au, "Powered ankle-foot prosthesis for the improvement of amputee walking economy," Thesis, Massachusetts Institute of Technology, 2007.
- [18] E. J. Rouse, L. M. Mooney, and H. M. Herr, "Clutchable series-elastic actuator: Implications for prosthetic knee design," *Int. J. Robot. Res.*, vol. 33, no. 13, pp. 1611–1625, Nov. 2014, doi: 10.1177/0278364914545673.
- [19] S. K. Au, J. Weber, and H. Herr, "Biomechanical Design of a Powered Ankle-Foot Prosthesis," in *2007 IEEE 10th International Conference on Rehabilitation Robotics*, Jun. 2007, pp. 298–303, doi: 10.1109/ICORR.2007.4428441.